The American Journal of Pathology, Vol. 178, No. 5, May 2011

DOI: 10.1016/j.ajpath.2011.01.016

Immunopathology and Infectious Diseases

The Neuropathology of Fatal Cerebral Malaria in Malawian Children

Katerina Dorovini-Zis,* Kristopher Schmidt,* Hanh Huynh,* Wenjiang Fu,† Richard O. Whitten,‡ Dan Milner,§ Steve Kamiza,§ Malcolm Molyneux,¶‖ and Terrie E. Taylor§**

From the Division of Neuropathology, Department of Pathology and Laboratory Medicine, Vancouver General Hospital and University of British Columbia, Vancouver, British Columbia, Canada; the Departments of Epidemiology,† and Internal Medicine,** College of Osteopathic Medicine, Michigan State University, East Lansing, Michigan; CellNetix Pathology,‡ Olympia, Washington; the Blantyre Malaria Project,§ and Malawi-Liverpool-Wellcome Trust Clinical Research Program,¶ College of Medicine, University of Malawi, Blantyre, Malawi; and the School of Tropical Medicine,‖ University of Liverpool, Liverpool, United Kingdom*

We examined the brains of 50 Malawian children who satisfied the clinical definition of cerebral malaria (CM) during life; 37 children had sequestration of infected red blood cells (iRBCs) and no other cause of death, and 13 had a nonmalarial cause of death with no cerebral sequestration. For comparison, 18 patients with coma and no parasitemia were included. We subdivided the 37 CM cases into two groups based on the cerebral microvasculature pathology: iRBC sequestration only (CM1) or sequestration with intravascular and perivascular pathology (CM2). We characterized and quantified the axonal and myelin damage, blood-brain barrier (BBB) disruption, and cellular immune responses and correlated these changes with iRBC sequestration and microvascular pathology. Axonal and myelin damage was associated with ring hemorrhages and vascular thrombosis in the cerebral and cerebellar white matter and brainstem of the CM2 cases. Diffuse axonal and myelin damage were present in CM1 and CM2 cases in areas of prominent iRBC sequestration. Disruption of the BBB was associated with ring hemorrhages and vascular thrombosis in CM2 cases and with sequestration in both CM1 and CM2 groups. Monocytes with phagocytosed hemozoin accumulated within microvessels containing iRBCs in CM2 cases but were not present in the adjacent neuropil. These findings are consistent with a link between iRBC sequestration and intravascular and perivascular pathology in fatal pediatric CM, resulting in myelin damage, axonal injury, and breakdown of the BBB. ***(Am J Pathol 2011, 178:2146–2158; DOI: 10.1016/j.ajpath.2011.01.016)***

Cerebral malaria (CM) is a serious complication of *Plasmodium falciparum* infection. Cerebral involvement occurs in approximately 1% of infected individuals and carries a 15% to 20% case-fatality rate, resulting in three-fourths of 1 million to 2 million deaths/year.[1] Young children in sub-Saharan Africa account for 90% of CM-associated deaths. Pediatric CM is a diffuse encephalopathy characterized clinically by deep coma, often associated with clinical or subclinical seizures in the presence of *P. falciparum* parasitemia. Most children who survive CM appear to fully recover, but 10% to 20% are left with neurological disabilities, most commonly spasticity, ataxia, hemiplegia, speech disorders, and blindness[2]; long-term sequelae, including cognitive impairment and epilepsy, are being identified with increasing frequency in follow-up studies.[3] The pathogenesis of coma in pediatric CM is poorly understood, and it is not known what mechanisms determine the outcome of the illness. Several pathogenetic mechanisms have been proposed, including impaired tissue perfusion because of sequestration of parasitized erythrocytes, immune-mediated injury secondary to host responses to parasite products, and cerebral edema resulting from increased permeability of the blood-brain barrier (BBB).[4–6] The relative contributions of these mechanisms to the final outcome of CM remain to be determined.

Previous neuropathological studies in adult patients with CM have documented the presence of axonal injury[7] and BBB dysfunction,[8] in addition to the typical pathological features of the disease that include adhesion and sequestration of *P. falciparum*–infected red blood cells (iRBCs) in brain microvessels, ring hemorrhages (RHs), and Dürck's granulomas. However, the syndrome of CM

Supported by grants from the National Institutes of Health (5RO1AI34969-12) and The Wellcome Trust, London, United Kingdom (074124/Z).

Accepted for publication January 7, 2011.

Address reprint request to Katerina Dorovini-Zis, M.D., Division of Neuropathology, Department of Pathology and Laboratory Medicine, Vancouver General Hospital, 855 W 12th Ave, Vancouver, British Columbia, Canada V5Z 1M9. E-mail: dorovini@interchange.ubc.ca.

in children is different from that in adults; therefore, extrapolations from one to the other regarding the pathophysiological characteristics of severe malarial infection are not possible. There is accumulating evidence that within cerebral vessels, adherent iRBCs induce endothelial activation, with several consequences. These include morphological changes[9] and increased expression of the endothelial cell adhesion molecules inter-cellular adhesion molecule 1 (ICAM-1), vascular cell adhesion molecule 1 (VCAM-1), and E-selectin.[10–12] An associated decreased expression of the tight junction–associated proteins occludin, vinculin, and zonula occludens protein 1 (ZO-1)[13] is likely to be associated with increased permeability of the BBB. These observations are supported by *in vitro* studies of cultured endothelial cells derived from human brain microvessels. Exposure of such monolayers to iRBCs leads to up-regulation of ICAM-1 expression, probably through nuclear translocation of NF-κB.[14] When using similar cell cultures, both membrane-associated and soluble iRBC factors can significantly reduce the barrier function of the endothelial monolayers.[15] Several studies[4,16–25] investigating the role of immune responses in CM have implicated both proinflammatory [tumor necrosis factor (TNF)-α, interferon-γ, IL-1β, and IL-6] and anti-inflammatory (IL-10 and transforming growth factor-β) cytokines and certain chemokines in disease pathogenesis; however, their pathophysiological and immunoregulatory roles in human CM are not fully understood.

A key issue in the pathogenesis of pediatric CM is the nature of tissue injury that leads to severe central nervous system (CNS) damage and death in some of the infected children. A detailed postmortem evaluation of cerebral microvessel sequestration in fatal pediatric CM has shown the presence of parasitized RBC sequestration in all patients with CM and an association of sequestration with microvascular pathology in 75% of these patients.[26] That study further suggested that some children with clinically diagnosed CM actually die of other causes. The presence of malarial retinopathy on funduscopic examination distinguished between malarial and nonmalarial coma during life.

In an attempt to better understand the pathophysiological events in fatal CM, we performed a detailed postmortem examination of the brains of 37 Malawian children with clinically and pathologically defined CM and compared the neuropathological findings with those in 13 cases of clinically defined CM (including *P. falciparum* parasitemia) but with an autopsy-identified nonmalarial cause of death and with the findings in 18 children who died of nonmalarial causes without evidence of peripheral parasitemia. The results of the study show that sequestration of parasitized RBCs and microvascular pathology are associated with extensive myelin and axonal damage, BBB breakdown, and glial responses in patients with fatal CM.

Materials and Methods

Patient Selection

We studied the brains of 50 Malawian children who died of clinically defined CM at the Pediatric Research Ward, Queen Elizabeth Hospital, Blantyre, Malawi. The clinical diagnostic criteria included the following: i) unrousable coma [Blantyre coma score $\leq$2 (of a possible 5)] with no improvement within 2 hours of admission, despite correction of hypoglycemia and treatment of seizures; ii) *P. falciparum* parasitemia; and iii) exclusion of other clinically identifiable causes of coma, including bacterial meningitis. These patients were further subdivided into three groups on the basis of the pathological characteristics of the cerebral microvasculature: CM1 (n = 7), CM2 (n = 30), and CM3 (n = 13). CM1 patients had iRBC sequestration within cerebral microvessels without other changes on routine histological examination of H&E-stained sections. In the CM2 group, RBC sequestration was associated with the presence of microvascular pathology and manifested on light microscopy as intravascular microthrombi and perivascular hemorrhages. There was no history of head trauma in any of the CM1 or CM2 patients. The patients classified as CM3 had no sequestration of parasitized erythrocytes in cerebral vessels. The pathological diagnoses of this group included pneumococcus pneumoniae (n = 2), pneumococcus pneumoniae and Reye's syndrome (n = 2), viral pneumonia and Reye's syndrome (n = 2), hepatitis (n = 1), hepatic necrosis (n = 1), giant-cell myocarditis (n = 1), ruptured arteriovenous malformation (n = 1), subdural and intracerebral hematomas (n = 1), severe anemia (n = 1), and cerebral edema, likely secondary to septicemia or hypoglycemia (n = 1). CM3 patients represented a cohort with CM symptoms but without malarial cerebral disease and only with incidental parasitemia. We added to this group a second cohort of 18 patients with CM symptoms but without CM and without parasitemia. These patients died of illnesses causing coma, had no peripheral parasitemia, and were described as "coma of other cause" (COC). These included bacterial or tuberculous meningitis (n = 3), viral encephalitis and Reye's syndrome (n = 1), sepsis (n = 4), sepsis and Reye's syndrome (n = 1), bacterial meningitis and Reye's syndrome (n = 1), Reye's syndrome (n = 3), salicylate toxicity (n = 1), organophosphate toxicity (n = 1), acute renal failure (n = 1), small-bowel obstruction (n = 1), and coma of unknown etiology (n = 1). Testing for HIV was performed in all cases using two rapid tests (Determine and Unigold). Discordant results would be addressed via PCR, but there were no discordant results in this series. In all cases, the patient was discovered to be HIV positive after admission to the research ward. None of these patients was receiving antiretroviral therapy at admission.

We performed a complete autopsy on all patients in the mortuary of Queen Elizabeth Hospital using a standardized dissection and collection protocol, after obtaining informed consent from the families of the deceased. The study was approved by the ethics committees of the College of Medicine, University of Malawi, Blantyre, Malawi; Michigan State University, East Lansing, MI; University of Liverpool, London, UK; and University of British Columbia, Vancouver, BC, Canada. At each autopsy, the brains were removed, photographed, weighed, examined, and sectioned in the fresh state. Representative sections from the frontal, parietal, temporal, and occipital

lobes; hippocampus; basal ganglia; thalamus; midbrain; pons; medulla; and cerebellum were fixed in 10% buffered formalin and embedded in paraffin. For analytical purposes, we grouped the representative sections as follows: white matter and gray matter from cerebral hemispheres (frontal, parietal, temporal, and occipital lobes and hippocampus), subcortex (caudate nucleus and thalamus), brainstem (midbrain, pons, and medulla), and cerebellum (tonsils and dentate nucleus).

Neurohistological Characteristics and Immunohistochemistry

Sections, 6-μm thick, were stained with H&E and Luxol fast blue/H&E. Sections, 3-μm thick, were stained with the indirect immunoperoxidase technique for the following: i) β-amyloid precursor protein (β-APP; 22C11, 1:500, mouse monoclonal; Chemicon, Temecula, CA) for the detection of axonal injury; ii) fibrinogen (1:500, rabbit polyclonal; Dako, Carpinteria, CA) for the assessment of BBB disruption; iii) glial fibrillary acidic protein (1:2000, rabbit polyclonal; DAKO) for the assessment of gliosis; iv) CD45 (2B11$^+$PD7/26, 1:100, mouse monoclonal; DAKO), CD68 (KP1, 1:60, mouse monoclonal; DAKO), CD8 (C8/144B, 1:80, mouse monoclonal; DAKO), and CD4 (1F6, 1:50, mouse monoclonal; NoVoCASTRA, Newcastle upon Tyne, UK) for the demonstration of leukocytes, monocytes, and CD8$^+$ and CD4$^+$ T lymphocytes, respectively; and v) CR3/43 (1:300, mouse monoclonal; DAKO) for the demonstration of class II major histocompatibility molecules (MHCs). Sections were deparaffinized by heating at 37°C overnight, then 60°C for 30 minutes, followed by three changes in xylene, two changes in 99% ethanol, one change in 95% ethanol, and several changes in water. Microwave antigen retrieval was performed in 10 mmol/L sodium citrate buffer for fibrinogen, β-APP, CD45, and CD68. Tris/EDTA buffer was used for CD8 and CD4 staining. After blocking the endogenous peroxidase, sections were incubated with 5% bovine serum albumin in Tris–Tween 20 buffer at room temperature for 30 minutes and incubated with the primary antibodies for 60 minutes (fibrinogen) or 90 minutes (glial fibrillary acidic protein, β-APP, CD45, and CD68) or overnight at 4°C (CD8 and CD4). After washing in Tris–Tween 20 buffer, sections were incubated for 1 hour with the secondary antibodies (goat anti-mouse or goat anti-rabbit IgG conjugated to horseradish peroxidase) at a 1:500 dilution, incubated in 3-amino-9-ethylcarbazole, and counterstained with hematoxylin. Negative controls included omission of primary antibodies and sections of age-matched normal brain specimens obtained from the Department of Pathology, BC Children's Hospital (Vancouver, BC, Canada). In the β-APP–stained sections, positive immunoreactivity of neuronal perikarya served as the positive control. Paraffin sections of tonsils or lymph nodes served as positive controls for CD4, CD8, CD45, CD68, and class II MHC staining.

Quantitative Evaluation of Neuropathological Findings

We quantified RHs by counting the number of hemorrhages in 10 randomly selected fields in each of the 12 sections with a microscope (Nikon Labophot) at $\times$10 magnification using a 1-cm^2 ocular grid. Myelin and axonal damage was similarly quantified by counting the number of white matter areas with myelin pallor and vacuolation and the number of foci with β-APP–positive swollen axons, with and without associated RHs in 10 randomly selected fields, in each section at $\times$10 magnification. In addition, the size of the areas with myelin or axonal damage was measured using the same 1-cm^2 ocular grid at $\times$10 magnification and expressed as micrometer squared areas of myelin or axonal damage per 10 fields. Quantification of fibrinogen leakage was performed by counting the number of leaky vessels in 10 randomly selected fields in the gray and white matter in each section at $\times$10 magnification. Gliosis was quantified by counting the number of reactive astrocytes in 10 randomly selected fields in each section at $\times$20 magnification using the ocular grid. The identity of the slides was masked before counting, so that all counts were performed by readers (authors K.S. and H.H.; and Farrah Samadi-Bahrami) who were unaware of the patient's clinical or pathological diagnoses.

Statistics

The four patient groups were described at baseline and had their characteristics compared through χ^2 and Fisher's exact tests when studying categorical measures and analysis of variance or the Kruskal-Wallis test when studying continuous measures. When appropriate, logarithmic transformations were performed and geometric means were estimated.[27] We were particularly interested in comparisons of CM1 with CM2 and with patients without malarial cerebral disease (CM3 and COC) because we wanted to identify alterations particular to malarial disease.

To characterize brain damage using previously described pathological counts, we summarized all count variables using medians of 10 randomly selected fields of each of the 12 brain areas: white and gray matter from cerebral hemispheres (frontal, parietal, temporal, and occipital lobes and hippocampus), subcortex (caudate and thalamus), brainstem (midbrain, pons, and medulla), and cerebellum (tonsils and dentate nucleus). Medians were estimated for each CM class separately, focusing on comparisons of CM1 and CM2 counts between brain regions.

Results

The patients in the four histopathologically defined groups (CM1, CM2, CM3, and COC) were essentially similar in age, duration of illness before and after admission, depth of coma on admission, and postmortem interval (Table 1). The CM1 and CM2 patients had, on

Table 1. Clinical and Demographic Features

Variable	CM1 (n = 7)	CM2 (n = 30)	CM3+COC (n = 31)	P value	CM3 (n = 13)	COC (n = 18)
Age (months)	56	42	41	0.49	33	48
Male sex (%)	29	63	45	0.19	69	28
HIV positive (%)	43	13	15	0.19	8	20
Blantyre Coma Score on admission	1.43	0.97	0.90	0.20	0.69	1.06
Admission parasitemia (geometric mean)	56,629	73,369	5450	0.02	5450	0
Coma duration before admission (hours)	7.20	11.36	10.00	0.65	5.50	5.50
Time to death (hours)	16.00	13.87	28.21	0.13	29.38	27.36
Autopsy interval (hours)	7.33	6.81	7.91	0.63	7.27	8.37

Data are given as mean unless otherwise indicated. P values were estimated for comparisons of the CM1 group versus the CM2 group versus the CM3 plus the COC group, except when comparing parasitemia because, by design, patients in the COC group did not have parasitemia. When comparing for sex and HIV, we used the Fisher's exact test. For admission parasitemia, we used the Kruskal-Wallis statistic. For age, coma at and before admission, time to death, and autopsy interval, we used analysis of variance.

average, higher-density peripheral blood parasitemias on admission compared with patients with nonmalarial cerebral disease (CM3 and COC). Results were essentially similar when the group of patients with nonmalarial cerebral disease was separated into CM3 and COC and comparisons were performed of CM1 versus CM2 versus either CM3 or COC. For instance, the P value of the Fisher's exact test comparing the four groups of patients on HIV-positive status was 0.23.

Gross Pathological Features

Gross examinations of the brains were performed in the fresh state. The brain weights were compared with the average normal brain weights of age-matched white children[28] because there are no published data on normal brain weights of African children. The brain weight of 21 of 30 CM2 cases was variably increased up to 32% higher than the normal weight (Figure 1). Of the remaining CM2 cases, seven had normal and two had slightly below normal brain weights. Among the seven CM1 patients, six had increased brain weights up to 51% above normal and one had a brain weight that was within normal limits. Of the 13 CM3 cases, eight had increased brain weights up to 27% higher than the normal range. In 14 of the 18 COC cases, the brain weight was increased; in

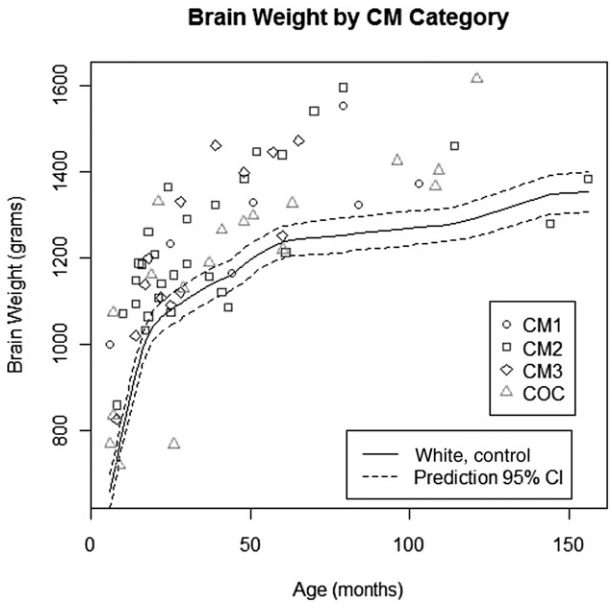

Figure 1. Brain weights of children in the CM1, CM2, CM3, and COC groups compared with the normal brain weights of age-matched white children. The brain weights of most children in the CM1, CM2, and, to a lesser extent, CM3 groups are higher than the normal values. CI indicates confidence interval.

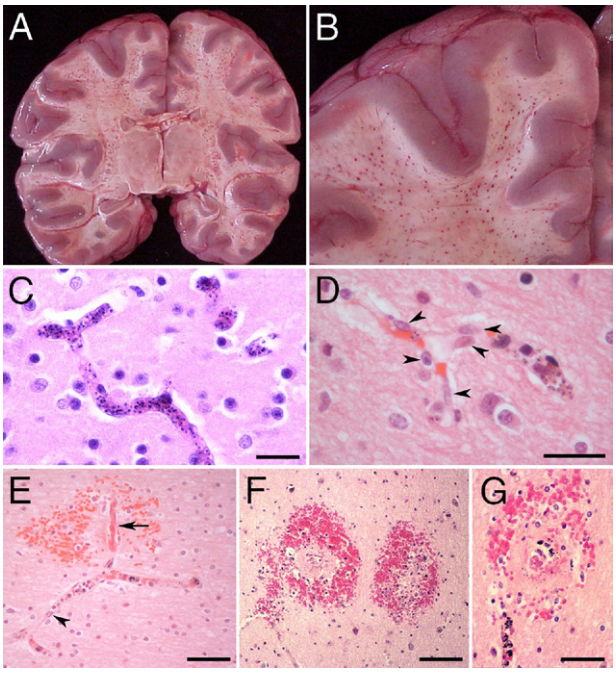

Figure 2. **A** and **B:** Coronal sections through the cerebral hemispheres of a CM2 patient. **A:** Numerous petechial hemorrhages are distributed throughout the white matter. The lateral and third ventricles are compressed because of edema. **B:** Close-up view of hemorrhages in the white matter. The gray matter is largely spared. **C** through **G:** Vascular changes in CM2 patients. **C:** The lumen of all small vessels in the field is distended by sequestered iRBCs. **D:** Some microvascular endothelial cells are hypertrophic and display large vesicular nuclei (**arrowheads**). **E:** A small branching vessel in the white matter contains iRBCs and hemozoin. One of the branches (**arrow**) is occluded by thrombus, is partially denuded of endothelial cells, and is associated with an RH. In the adjacent branch with iRBC sequestration, hypertrophic endothelial cells display large nuclei (**arrowhead**). **F** and **G:** RHs in the cerebral white matter correspond to petechial hemorrhages in **A** and **B**. **G:** Small, often thrombosed, ruptured capillaries containing iRBCs are immediately surrounded by a zone of necrosis that, in turn, is surrounded by a ring of extravasated RBCs, a few white blood cells, and extraerythrocytic pigment granules. **C** through **G:** H&E staining. Scale bars: 25 μm (**C** and **D**); 50 μm (**E** and **G**); 100 μm (**F**).

three cases, it was within the normal range; and in one case, the brain weight was lower than normal. There was a variable degree of flattening of the gyri and narrowing of the sulci in patients with brains of increased weight. Among the children with a significantly increased brain weight, mild tonsillar and/or uncal herniation was observed in 10 (six in the CM2, two in the CM1, one in the CM3, and one in the COC group). Coronal sections of the brains of all CM2 patients showed the presence of numerous petechial hemorrhages widely distributed in the white matter of the cerebral hemispheres (Figure 2, A and B), in the brainstem, and in the white matter of the cerebellum, including the cerebellar folia.

Histopathology—Sequestration and Microvascular Pathology

In both CM1 and CM2 patients, most microvessels in the gray and white matter contained sequestered iRBCs (Figure 2C). In larger pial and subarachnoid vessels, iRBCs were adherent to the endothelium without occupying the entire lumen. Independent of the presence or absence of iRBC sequestration, microvessel endothelial cells often appeared hypertrophic, with prominent vesicular nuclei (Figure 2D). Sequestration in the CM2 group was frequently associated with fibrin–platelet thrombi and intravascular accumulation of pigment–containing monocytes (Figure 2E). Microvascular thrombosis was often associated with necrosis of the endothelial lining of the occluded vessel and perivascular hemorrhage (Figure 2E).

Perivascular RHs, characterized by a central, often thrombosed, ruptured capillary containing iRBCs and surrounded by a zone of necrosis with an outer ring of extravasated nonparasitized RBCs and a few white blood cells, were a feature of CM2, but not (by definition) of CM1, patients (Figure 2, F and G). In the cerebral hemispheres, these hemorrhages invariably occurred in the white matter, with extension to the gray–white matter junction, but were rare in the cortical and subcortical gray matter. RHs were most numerous in the cerebral hemispheres, brainstem, and cerebellum, followed by the subcortex (Figure 3A). There was no sequestration and no intravascular or perivascular pathological features in the CM3 and COC groups.

Myelin and Axonal Injury

Myelin damage was assessed in sections stained with Luxol fast blue/H&E. Two different types of myelin damage were observed. The first type was characterized by discrete areas of total myelin loss in the necrotic perivascular zone of RHs (Figure 4A). The second type consisted of patchy, poorly defined, irregular, diffuse, and variably sized foci of myelin pallor and vacuolation associated with prominent sequestration of iRBCs within capillaries at the center of these foci (Figure 4, B and C). Neither of these lesions was associated with phagocytosis of myelin by macrophages. RH–associated myelin loss was a feature of CM2 cases and followed the distribution of RHs (Figure 3B). Areas of diffuse myelin damage were present in both the CM1 and CM2 groups. These areas were distributed in the white matter of the cerebral hemispheres and cerebellum and in the white matter tracts of the subcortex and brainstem in the CM2 group but were found only in the white matter of the cerebral hemispheres, subcortex, and brainstem in the CM1 group (Figure 5A). The largest areas of diffuse myelin damage were observed in the cerebral hemispheres and cerebellum of the CM2 cases and the smallest areas in the brainstem. In the CM1 cases, the largest areas of myelin pallor and vacuolation were in the brainstem and the smallest areas were in the white matter of the cerebral hemispheres. Diffuse myelin damage was the most common type of myelin pathology and was found even in

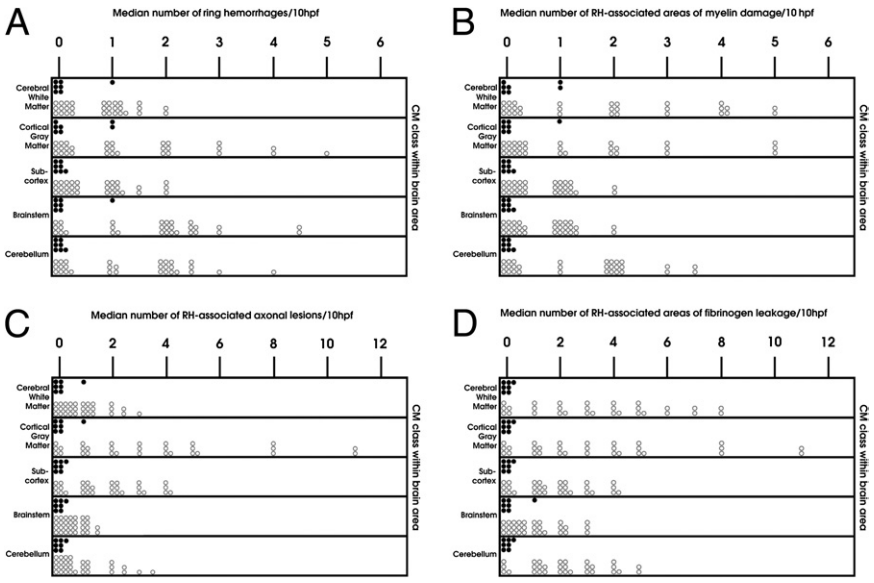

Figure 3. Quantification of RHs (**A**) and RH-associated findings (**B–D**) in the CM1 (shaded circles) and CM2 (unshaded circles) groups. **A:** The RHs are present only in the CM2 group and are most numerous in the cerebral white matter, followed by the cerebellar white matter, brainstem, and fiber tracts of the subcortical gray matter. In the cortex, RHs occur at the gray-white matter junction. **B:** RH-associated myelin damage is confined to the CM2 group and follows the distribution of RHs, being most frequent in the cerebral white matter and gray-white matter junction, followed by the cerebellar white matter and the fiber tracts of the subcortical gray matter and brainstem. **C:** RH-associated axonal injury occurs only in the CM2 group, follows the distribution of RHs, and is most prevalent in the cerebral and cerebellar white matter and the fiber tracts of the subcortical gray matter, followed by the brainstem. **D:** Fibrinogen extravasation in association with RHs is confined to CM2 cases, follows the distribution of these hemorrhages, and is most prevalent in the cerebral white matter, followed by the cerebellum, subcortex, and brainstem. hpf indicates high-power field.

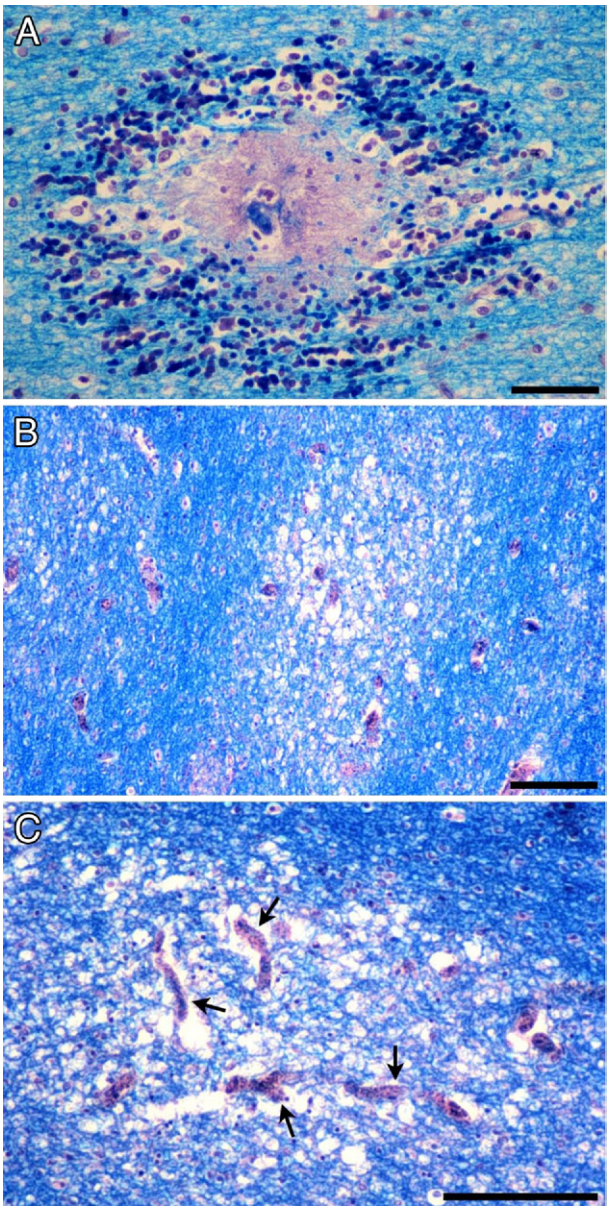

Figure 4. Myelin damage in pediatric CM. **A:** Myelin pallor and fragmentation has occurred in association with an RH surrounding a thrombosed and disrupted parasitized microvessel in the cerebral white matter. **B:** Irregular, ill-defined, and variably sized foci of diffuse myelin vacuolation and pallor unassociated with RHs typically occur in the CM2 and, to a lesser extent, CM1 groups. **C:** Areas of diffuse myelin damage encompass several distended microvessels filled with iRBCs (**arrows**). Luxol fast blue/H&E staining. Scale bars: 50 μm (**A**); 100 μm (**B** and **C**).

cases with few or no RHs. RH–associated myelin loss was not present in either CM3 or COC cases. Occasional small foci of diffuse myelin pallor were found in the cerebral white matter and rarely in the brainstem and cerebellum of a few CM3 cases but not in the COC group.

Axonal injury was assessed by staining sections with the indirect immunoperoxidase technique for β–APP, an axonally transported protein that accumulates within injured axons as a result of disruption of the fast axonal transport in various CNS disorders. It is a reliable, sensitive, and early marker for axonal injury that can be detected within 2 to 3 hours[29,30] and as early as 35 minutes after injury.[31] Axonal β-APP is not detectable in the normal brain by routine IHC of FFPE sections. Three distinct types of axonal injury were observed. The first type was associated with RHs in CM2 patients and consisted of variably sized clusters of intensely β-APP–immunoreactive swollen and disrupted axons with axonal spheroid formations immediately adjacent to the hemorrhage (Figure 6A). The number of hemorrhage-associated β-APP–positive axons varied even within the same section. Some RHs were associated with only occasional abnormal axons, suggesting a <1-hour interval between the occurrence of the hemorrhage and death (Figure 6B). The distribution of this type of axonal damage followed that of RHs, being most prevalent in the white matter of the cerebral hemispheres, followed by the fiber tracts of the subcortex and the cerebellar white matter, and least common in the brainstem (Figure 3C). The second type of axonal injury consisted of patchy, ill-defined, irregular, discrete or confluent, variably sized collections of closely packed strongly β-APP–positive tortuous axons with varicosities and focal swellings along their course. These areas of axonal injury were not associated with hemorrhage and were randomly distributed in the white matter of the cerebral and cerebellar hemispheres (Figure 6, C–F) and in fiber tracts of the basal ganglia, thalamus, pons (Figure 6G), midbrain, and medulla (Figure 6H) in CM1 and CM2 patients. This type of diffuse axonal damage was often associated with capillaries packed with sequestered iRBCs in the center of the lesion (Figure 6, F and G). Diffuse axonal injury was not evenly distributed in the CNS and was most frequent in the cerebral hemispheres, brainstem, and cerebellum and least frequent in the subcortex. The largest areas of diffuse axonal damage were in the cerebral and cerebellar white matter, whereas the smallest foci were present in the medulla (Figure 5B). Diffuse axonal damage was not confined to CM2 cases but was also present in CM1 cases, although both the number and size of these lesions were smaller in CM1 than in CM2 cases (Figure 5B). Some CM3 cases showed infrequent, single, β-APP–positive axons scattered in the white matter tracts of the brainstem. Diffuse axonal damage was the most frequent type of axonal injury and was present even in cases with few or no RHs. Axonal damage was not present in the COC group of patients. The third type of axonal damage was characterized by small discrete foci of β-APP immunoreactivity immediately adjacent to a capillary containing parasitized RBC and fibrin-platelet thrombi (Figure 6, I and J) without an associated RH. This was the least common type of axonal injury and was observed only in CM2 patients. In sections double stained for β-APP and Luxol fast blue, diffuse myelin damage often coincided with diffuse axonal injury; however, there were areas of myelin loss devoid of β-APP–positive axons (Figure 6, K and L). In contrast, axonal injury was invariably associated with myelin changes.

BBB Permeability

The permeability of the BBB was assessed by immunostaining sections for fibrinogen, a 340,000 mol.wt. serum

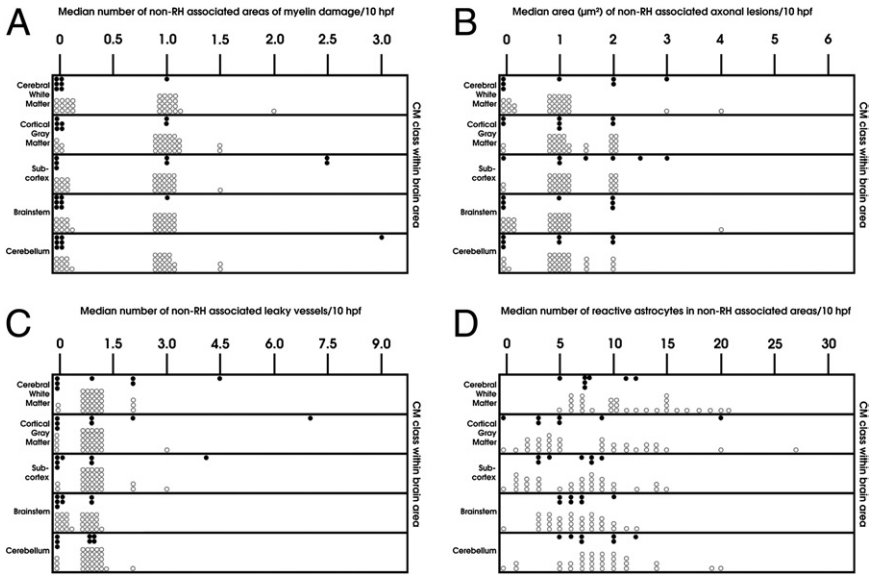

Figure 5. Quantification of non–RH-associated damage in the CM1 (shaded circles) and CM2 (unshaded circles) groups. **A:** Areas of diffuse myelin damage are present predominantly in CM2 and, to a much lesser extent, CM1 patients and are only occasionally found in the nonmalarial groups. **B:** Diffuse axonal injury is present in both CM2 and CM1 patients, with only occasional small lesions seen in the CM3 and COC groups. The largest areas of axonal damage occur in the cerebral and cerebellar white matter, followed by the subcortex and brainstem. **C:** Increased permeability to fibrinogen, independent of RHs or thrombosis, is present in the two malaria groups (CM1 and CM2), with no significant differences between the two groups. **D:** Reactive astrocytes are present in the subcortical and deep white matter of all brain regions examined in both CM1 and CM2 patients. Compared with the CM1 class, the CM2 group exhibits a greater degree of gliosis in the cerebral white matter. hpf indicates high-power field.

protein that is normally excluded from the brain by the intact BBB.[32] In CM, increased permeability of the BBB was usually, but not exclusively, associated with specific vascular pathological features, so that three patterns of BBB breakdown could be distinguished. The first pattern was characterized by fibrinogen extravasation in association with RHs (Figure 7A) and was confined to the white matter of the cerebral hemispheres, subcortex, brainstem, and cerebellum in the CM2 cases (Figure 3D). The second pattern consisted of fibrinogen leakage around microvessels occluded by fibrin thrombi (Figure 7B) in the white matter and, to a lesser extent, the gray matter of the cerebral hemispheres, brainstem, and cerebellum in CM2 patients. In the third type of BBB breakdown, fibrinogen was deposited around blood vessels with prominent RBC sequestration but without fibrin thrombi, in both CM1 and CM2 patients, following the same distribution as the second type of lesions (Figure 5C and Figure 7, C and D). In addition, scattered leaky vessels without associated vascular pathological features were present in all CM1 and CM2 cases. Focal extravasation of fibrinogen across cortical and white matter microvessels was also observed in the CM3 and COC groups, without associated vascular wall changes or intravascular pathology. When the overall number of leaky vessels was considered, there were no significant differences in BBB disruption among the four groups of patients. However, the number of permeable parasitized vessels in the subcortex and brainstem was greater in the CM2 than the CM1 cases (Figure 5C). The number of vessels permeable to fibrinogen was greater in the white matter than in the gray matter in all patient groups, with the exception of the COC patients, in whom no significant differences were found.

Cellular Immune Responses

A consistent finding in all malaria cases was the absence of an extravascular localized immune response to the vascular, myelin, and axonal pathology. Dürck's granulomas, which consist of collections of reactive microglia, astrocytes, and lymphocytes, were not present in any of the 37 cases of CM. Dürck's granulomas are a feature of adult CM and probably represent a later immune response to focal parenchymal necrosis. A variable number of CD45/CD68-positive monocytes containing hemozoin were present in the lumen of microvessels in the gray and white matter of the cerebral hemispheres, subcortex, brainstem, cerebellum, and leptomeninges of CM2 patients. Microvessels were often distended by the accumulated monocytes, which appeared to occupy most of the lumen of capillaries and venules but did not migrate out of the vessels into brain tissue (Figure 8, A, C, and D). Often, a capillary lumen was completely filled with a (presumably adherent) monocyte (Figure 8, A, C, and D). Monocytes with phagocytosed malarial pigment were usually present, along with extravasated RBCs, in the center of RHs (Figure 8B). Neither $CD4^+$ nor $CD8^+$ T lymphocytes were found in areas of RH, myelin, or axonal damage in CM1 or CM2 cases; and only occasional $CD8^+$ T cells were observed within the vascular lumen and, infrequently, in the subendothelial region of a few blood vessels in one CM1 and three CM2 cases. Scattered perivascular chronic inflammatory cell infiltrates were present in the brain parenchyma in some of the infectious CM3 cases. Occasional microglial cells expressing class II MHC molecules were seen in a few CM2 cases. Among the HIV-positive children, we did not observe pathological changes of HIV encephalitis or opportunistic infections.

Astrocytic Responses

We assessed the presence, severity, and distribution of gliosis in sections immunostained for glial fibrillary acidic protein. There was diffuse proliferation of reactive astrocytes in the subcortical and deep white matter of the cerebral hemispheres and cerebellum and along fiber tracts in the basal ganglia, thalamus, and brainstem in all CM1 and CM2 cases. Reactive astrocytes were not found

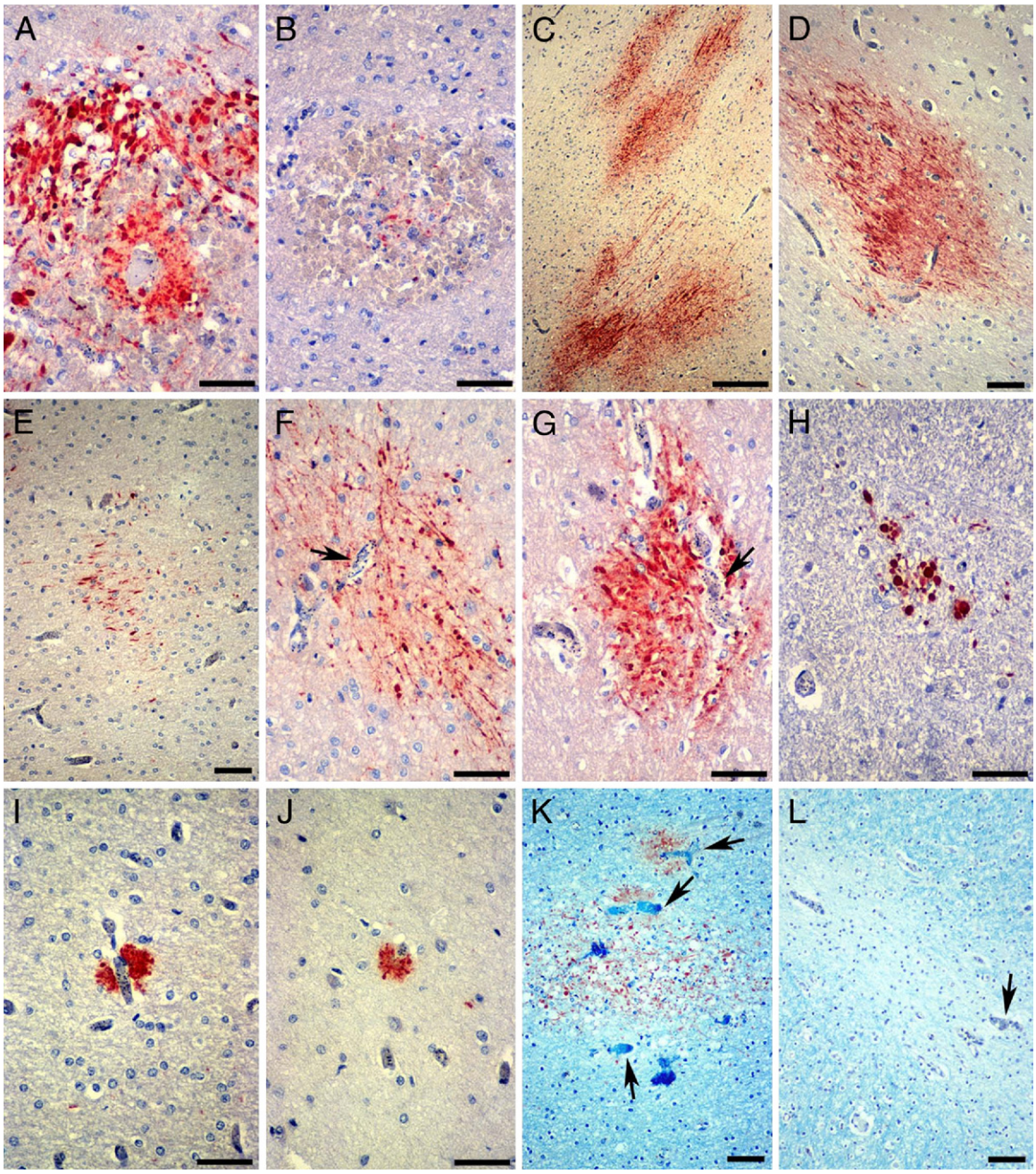

Figure 6. Patterns of axonal damage in pediatric CM detected by β-APP IHC. **A** and **B:** RH-associated axonal damage. **A:** Strongly β-APP–immunoreactive swollen and disrupted axons in an RH around a thrombosed and ruptured white matter capillary. **B:** Only a few β-APP–positive axons are present in the center of some RHs. **C** through **H:** Diffuse axonal injury in CM2 patients. Confluent (**C**) or single (**D**) ill-defined irregular patches of β-APP–immunoreactive axons in the cerebral and cerebellar white matter (**C**, **E**, and **F**), the gray-white matter junction (**D**), and pons (**G**). Diffuse axonal damage occurs in areas with heavy iRBC sequestration (**F** and **G**, **arrows**). **H:** Smaller diffuse lesions are evident in the medulla. **I** and **J:** Small discrete foci of β-APP–positive axons are present immediately adjacent to capillaries occluded by iRBC with (**I**) or without (**J**) a thrombus. In sections double stained for β-APP and Luxol fast blue, diffuse axonal and myelin lesions often (**K**), but not invariably (**L**), coincide in areas with prominent iRBC sequestration (**arrows**). Scale bars: 50 μm (**A**, **B**, and **F**–**J**); 250 μm (**C**); 100 μm (**D**, **E**, **K**, and **L**).

in the cortex, with the exception of mild focal subpial gliosis in a few cases. The degree of astrogliosis varied among the CM cases, from mild to moderate, and did not correlate with RBC sequestration or myelin or axonal damage. There was no spatial association between gliosis and either RHs or areas of axonal or myelin changes. Reactive astrocytes were present at a similar density in and around patches of axonal and myelin lesions (Figure 9A) and RHs (Figure 9B) as they were in the white matter that appeared uninvolved. Gliosis was not a unique feature of CM because all COC cases and 10 of the 13 CM3 cases showed comparable astrocytic responses. However, when comparing the different groups, gliosis was more prominent in the cerebral white matter of CM2 versus CM1 patients (Figure 5D) and in the cerebral white matter and brainstem of CM1 and CM2 cases than in the CM3 group.

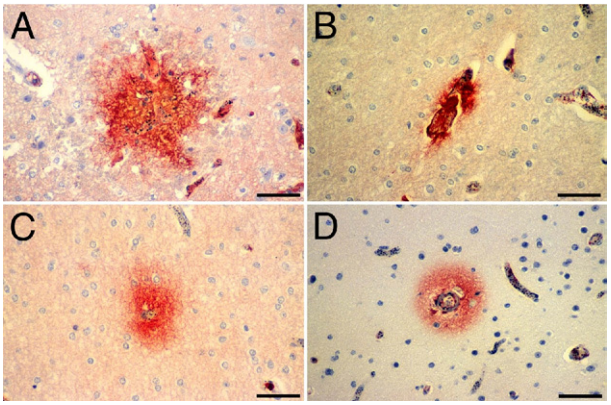

Figure 7. Patterns of BBB disruption detected by fibrinogen IHC. **A:** Fibrinogen extravasation occurs in association with ruptured capillaries and RHs. **B:** Fibrinogen has extravasated across a microvessel occluded by thrombus. **C** and **D:** Increased permeability of the BBB to fibrinogen in microvessels with heavy iRBC sequestration occurs without thrombosis or hemorrhage in the white (**C**) and gray (**D**) matter. Scale bar = 50 μm (**A**–**D**).

Discussion

In this study, we describe the brain pathological features in a large series of Malawian children dying of CM. We compare the neuropathological findings with those in children who met the standard case definition of CM during life but had no evidence of parasite sequestration in the cerebral microvasculature and had a nonmalarial cause of death identified at autopsy. As a further comparison group, we included children without malarial infection, who died with COC. Patients with clinically defined CM were classified into three groups based on the cerebral histological appearance on light microscopy: presence of sequestration of iRBCs only (CM1), sequestration with intravascular and perivascular pathology (CM2), and absence of sequestration (CM3).

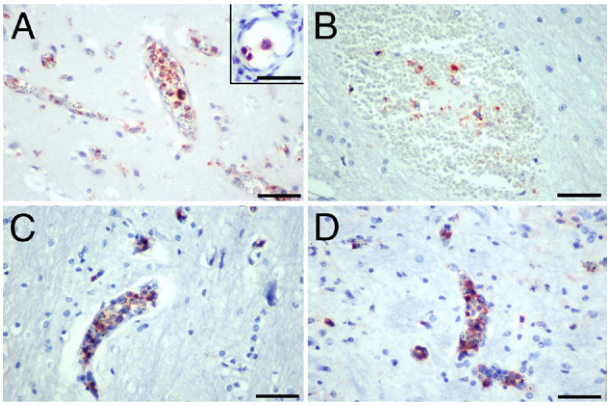

Figure 8. Immunohistochemical demonstration of intravascular monocytes in the CM2 group. Monocytes with phagocytosed extraerythrocytic pigment fill and distend the lumen of many small vessels in the cortex (**A**), pons (**C**), and medulla (**D**). Although adherent to the endothelium (**A**, **inset**), monocytes do not transmigrate across the BBB to infiltrate the neuropil. The lumen of several capillaries (**A**, **C**, and **D**) is occluded by adherent monocytes. **B:** Monocytes, along with pigment and RBCs, have been released from the vascular lumen in an RH. Stainings: CD68 (**A** and **B**); CD45 (**C** and **D**). Scale bars: 50 μm (**A**–**D**); 2 μm (**inset**).

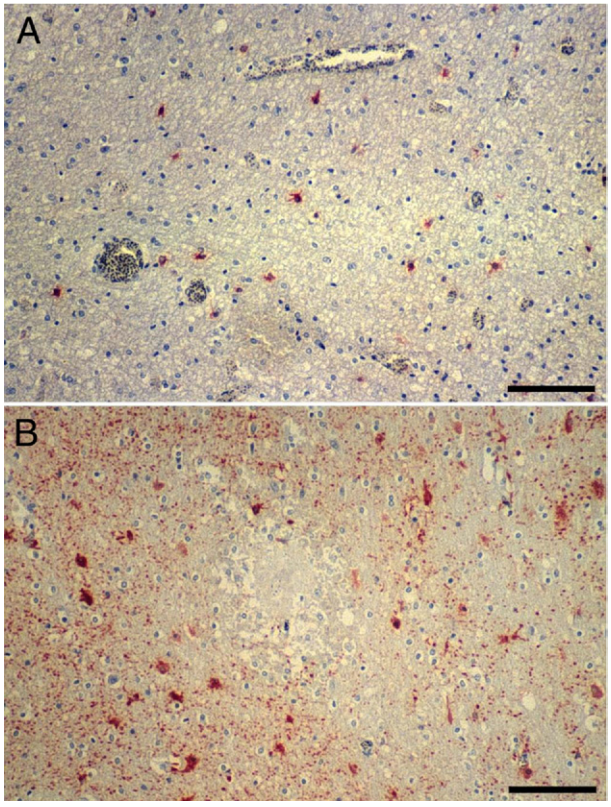

Figure 9. Reactive gliosis in CM detected by glial fibrillary acidic protein IHC. **A:** Mild diffuse gliosis in and around an area of myelin pallor and vacuolation and prominent iRBC sequestration. **B:** Diffuse gliosis in the neuropil around an RH. Scale bar = 100 μm (**A** and **B**).

On gross examination, a mild to moderate increase of brain weight was present in 6 (86%) of the CM1 cases, 21 (70%) of the CM2 cases, and 8 (62%) of the CM3 cases. The contribution of cerebral edema to the pathophysiological features and clinical outcome of CM is not well understood. Increased intracranial pressure (identified by computed tomography) and postmortem brain edema have been reported in African children with CM and are associated with poor prognosis.[33–35] In addition, some children with severe intracranial hypertension had widespread low-density areas on computed tomographic scans, suggestive of ischemic damage.[36] In contrast, postmortem studies[37] of adult patients with CM have shown the presence of cerebral edema in a few patients and do not support a direct link between brain swelling and fatal outcome. Several factors may contribute to cerebral edema, including RHs and increased permeability of the BBB. In view of differences in the pathological findings among our four patient groups, it is likely that more than one mechanism is responsible for the pathogenesis of cerebral edema in these patients.

All CM2 cases showed, by definition, significant vascular pathology in the form of iRBC sequestration in association with the presence of intraerythrocytic pigment and pigment granules in macrophages, RHs, and focal occlusion of the parasitized microvessels by fibrin-platelet thrombi. RHs, a pathological hallmark of CM, were present only in the CM2 cases and were most frequent in

the white matter of the cerebrum and cerebellum and, to a lesser extent, in the basal ganglia, thalamus, and brainstem. They surrounded heavily parasitized and often thrombosed microvessels that exhibited segmental loss of endothelial cells. These findings suggest that RHs are the result of irreversible endothelial damage and necrosis, leading to abrupt disruption of the endothelial lining and subsequent extravasation of nonparasitized RBCs, pigment globules, and macrophages. In the absence of local thrombosis, endothelial cells of parasitized vessels appeared normal or displayed large vesicular nuclei suggestive of activation.

Morphological alterations of brain endothelium at the site of iRBC sequestration have been described.[9] Several studies[38] provide evidence of endothelial activation and up-regulation of adhesion molecules, such as ICAM-1, VCAM-1, E-selectin, platelet endothelial cell adhesion molecule 1 (PECAM-1), thrombospondin, and chondroitin sulfate, that have been implicated in the cytoadherence of *P. falciparum* to the endothelium. In a recent study,[39] coincubation of human brain endothelial cell monolayers with *P. falciparum*–infected erythrocytes for 6 hours resulted in up-regulation of the NF-κB signaling pathway, induction of ICAM-1, and up-regulation of chemokines, cytokines, proapoptotic and antiapoptotic proteins, and genes related to the immune response. Although the exact mechanisms involved in the activation of the cerebral endothelium in our cases are not known, it is possible that contact-dependent or soluble parasite factors and circulating cytokines play a role. Under normal conditions, the vascular endothelium has a nonthrombogenic luminal surface that resists platelet adhesion and thrombosis. Exposure of endothelial cells to certain inflammatory mediators, such as IL-1β and TNF-α, induces procoagulant activity and tissue factor production and suppresses fibrinolytic activity.[40–43] It is likely that in CM, several factors, including circulating cytokines, locally released IL-1β and TNF-α, and mediators released from iRBCs or after iRBC lysis, act on the BBB endothelium to induce prothrombogenic changes on the luminal surface. The formation of fibrin thrombi, often in association with focal loss of endothelial cells and with RHs, suggests that there are critical alterations of endothelial function that could lead to irreversible endothelial damage. These observations are consistent with the results of recently reported *in vitro* studies that suggest that direct contact with iRBCs induces endothelial apoptosis through a caspase-dependent pathway[44] and that some *P. falciparum* strains are more apoptogenic than others.[45] A pathogenic role for platelets in endothelial damage has also been suggested in recent studies[46] showing that platelets potentiate the cytotoxic effect of iRBCs on brain endothelial cells through direct contact with the endothelium. The *P. falciparum*–associated molecules that induce endothelial activation versus apoptosis and the mechanisms involved are also not known.

RH-associated myelin and axonal damage was a prominent and constant finding in all CM2 cases. Physical damage of the myelin sheaths and axons, secondary to sudden disruption of the vessel wall and hemorrhage, seems to be the most likely pathogenetic mechanism. Not uncommonly, the area with myelin pallor and vacuolation surrounding RHs contained few, if any, β-APP–immunoreactive axons. Because β-APP IHC detects abnormal axons as early as 35 minutes after injury, the presence of RHs with myelin damage and only a few or no β-APP–positive axons suggests that these hemorrhages occurred shortly before death. Diffuse myelin and axonal damage in CM2 and CM1 cases occurred in areas with prominent iRBC sequestration in white matter capillaries and venules. Although close proximity of some of these areas to RHs in the CM2 cases cannot be entirely excluded, the size, shape, and distribution of these lesions strongly suggest that they are likely the result of anoxic injury secondary to microvascular occlusion by sequestered iRBCs and/or fibrin-platelet thrombi. This is supported by the presence of minute discrete axonal lesions immediately surrounding thrombosed capillaries and by the fact that diffuse axonal and, to a lesser extent, myelin damage was found in all CM1 cases in which RHs were entirely absent. Although diffuse myelin and axonal damage often coincided, the acute nature of these lesions, as indicated by the absence of reactive changes, suggests that they occurred independently of each other. To what extent the diffuse multifocal myelin and axonal lesions are reversible or permanent and associated with either a fatal outcome or neurological and cognitive deficits in the surviving patients is unknown. A somewhat different type of axonal injury was previously identified in adult Vietnamese patients dying of CM.[7] Similar foci of myelin and axonal damage can be seen in acute disseminated encephalomyelitis and as small perivascular lesions in intravascular lymphoma of the CNS around microvessels occluded by neoplastic lymphocytes.

Disruption of the BBB was present in all four patient groups and was associated with a different type of vascular pathology in each group of patients. Increased permeability to fibrinogen around RHs and thrombosed microvessels was a unique feature of CM2 patients. This type of BBB disruption is obviously secondary to irreversible endothelial damage and loss of the endothelial lining of the involved vessels and is likely one of the mechanisms contributing to cerebral edema. In both CM1 and CM2 cases, extravasation of fibrinogen occurred across several heavily parasitized microvessels without associated overt disruption of the endothelial lining. In the CM3 and COC cases, the increased permeability of the BBB was randomly distributed and was not associated with any specific vascular pathology. Previous postmortem studies[47] in eight Malawian children with CM showed focal loss of immunostaining for the endothelial tight junctional proteins ZO-1, occludin, and vinculin that spatially coincided with the presence of sequestered iRBCs in small vessels but was not associated with fibrinogen extravasation around these vessels. Studies in adult Vietnamese patients with CM by some of the same researchers[4] showed similar changes in the distribution of junctional proteins and, in addition, leakage of plasma proteins across cerebral microvessels.

The mechanisms responsible for the dysfunction of the BBB in pediatric CM have not been fully elucidated. The adhesion of sequestered iRBCs to cerebral endothelium

has been proposed as a contributing factor, and this hypothesis is supported by *in vitro* studies. These studies show decreased mRNA levels for tight junction proteins in endothelial cell monolayers co-cultured with iRBCs from CM patients[48] and decreased transendothelial electrical resistance of human brain endothelial cell monolayers on direct contact with *P. falciparum* iRBCs or *P. falciparum* iRBC culture supernatants, suggesting the involvement of both contact-dependent and contact-independent factors.[15] Cytokines, either locally or systemically released by activated macrophages, may further contribute to the increased permeability of the BBB. Incubation of human brain endothelial cell cultures with TNF-α, interferon-γ, or IL-1β induces morphological changes associated with increased permeability to horseradish peroxidase and decreased transendothelial electrical resistance across the monolayers.[49,50] The production of these cytokines by monocytes and $CD4^+$ T lymphocytes in response to iRBC and malarial pigment has been documented in CM[51,52] and may, at least in part, account for the increased permeability of the BBB in microvessels, with prominent sequestration in CM1 and CM2 cases and in CM3 and COC cases with an infectious etiology.

Invasion of the brain by T cells and macrophages and localized extravascular cellular immune responses were uniformly absent in CM1 and CM2 patients. The presence of hemozoin-laden monocytes within the lumen of small cerebral blood vessels was invariably associated with intravascular and perivascular pathology and further distinguished the CM2 group from the other patient groups. Although monocytes aggregated and adhered to the luminal surface of the endothelium, they remained intravascular and did not migrate across the vessel wall to enter the brain parenchyma. The only exception was the few extravasated monocytes in association with RHs. Monocyte adhesion to cerebral endothelium is mediated by interactions between ICAM-1 and VCAM-1, which have been shown to be up-regulated in CM,[10,11,53] and their corresponding ligands on monocytes, macrophage-1 antigen (MAC-1) (CD11β/CD18), and VLA4 (α4/β1).[54] ICAM-1 is a key molecule in the adhesion cascade and mediates both adhesion and transendothelial migration.[55] Therefore, it is intriguing that hemozoin-laden monocytes are found only within the microvessel lumen and do not appear to have migrated through or beyond the vessel wall. Experimental studies have shown that uptake of hemozoin results in both down-regulation of certain monocyte functions, such as class II MHC and integrin expression, oxidative burst, and repeat phagocytosis; and up-regulation of other functions, including the production of metalloproteinase 9, chemokines, and cytokines.[56] Phagocytosis of hemozoin and iRBC could potentially initiate intracellular events that would interfere with the formation of actin-rich filopodia, resulting in the inability of adherent monocytes to transmigrate. Alternatively, hemozoin and/or factors released from ruptured iRBCs may act on endothelial cells to inhibit "outside-in" signaling after ICAM-1 ligation and the formation of stress fibers, which are essential for cell migration.[57] Increased serum levels of the monocyte-produced macrophage migration inhibitory factor (MIF) and the *P. falciparum*–derived MIF homologue have been reported in patients with malaria.[58,59] Recent *in vitro* studies[60] showed that pretreatment of endothelial cells with MIF induces monocyte arrest through binding of MIF to the chemokine receptors CXCR2 and CXCR4. The presence of adherent intravascular monocytes could further reduce the already compromised capillary blood flow as a result of iRBC sequestration.

Our findings demonstrate several pathological changes in the brain in fatal pediatric CM. Some of these changes, such as brain edema and astrogliosis, appear not to be specific to malaria and are shared by nonmalarial fatal encephalopathies. Others, including RHs and diffuse axonal and myelin damage, were seen in children with CM and not in those who died of a nonmalarial illness. Changes that were most prominent and distinctive in malaria appeared to be located within and in the vicinity of blood vessels containing sequestered iRBCs, platelets, hemozoin pigment, or monocytes. Evidence of both activation and destruction of the endothelial cells lining microvessels was prominent among these changes. The most severe endothelial damage, commonly associated with intraluminal thrombosis, manifested as disruption of the vessel wall, with surrounding RH formation. Myelin and axonal damage was most evident in proximity to affected microvessels, suggesting that intravascular and extravascular pathological changes are linked in a causal sequence in CM. However, postmortem studies cannot confidently demonstrate sequence or causality among topographically associated pathological features, and further electrophysiological, biochemical, and imaging studies in prefatal and nonfatal CM are needed to further our understanding of how malaria causes coma, brain damage, and death.

Acknowledgments

We thank Farrah Samadi-Bahrami, Henry Lau, and Hong Li (KD-Z Neuropathology Research Laboratory, Vancouver General Hospital, Vancouver, BC, Canada) for their expert technical assistance with tissue sectioning and staining and with IHC; Annmarie Cook (Michigan State University, East Lansing, MI) for her expert help with graphics; and all of the nurses, laboratory technicians, and mortuary attendants in Blantyre, Malawi, who worked diligently in support of this effort.

References

1. World Health Organization, Communicable Diseases Cluster. Severe falciparum malaria. Trans R Soc Trop Med Hyg 2000, 94(Suppl 1): S1–S90
2. Murphy SC, Breman JG: Gaps in the childhood malaria burden in Africa: cerebral malaria, neurological sequelae, anemia, respiratory distress, hypoglycemia, and complications of pregnancy. Am J Trop Med Hyg 2001, 64:57–67
3. John CC, Bangirana P, Byarugaba J, Opoka RO, Idro R, Jurek AM, Wu B, Boivin MJ: Cerebral malaria in children is associated with long-term cognitive impairment. Pediatrics 2008, 122:e92–e99
4. Brown H, Turner G, Rogerson S, Tembo M, Mwenechanya J, Molyneux M, Taylor T: Cytokine expression in the brain in human cerebral malaria. J Infect Dis 1999, 180:1742–1746

5. MacPherson GG, Warrell MJ, White NJ, Looareesuwan S, Warrell DA: Human cerebral malaria: a quantitative ultrastructural analysis of parasitized erythrocyte sequestration. Am J Pathol 1985, 119:385–401
6. Medana IM, Chaudhri G, Chan-Ling T, Hunt NH: Central nervous system in cerebral malaria: "innocent bystander" or active participant in the induction of immunopathology? Immunol Cell Biol 2001, 79: 101–120
7. Medana IM, Day NP, Hien TT, Mai NT, Bethell D, Phu NH, Farrar J, Esiri MM, White NJ, Turner GD: Axonal injury in cerebral malaria. Am J Pathol 2002, 160:655–666
8. Medana IM, Turner GD: Human cerebral malaria and the blood-brain barrier. Int J Parasitol 2006, 36:555–568
9. Pongponratn E, Turner GD, Day NP, Phu NH, Simpson JA, Stepniewska K, Mai NT, Viriyavejakul P, Looareesuwan S, Hien TT, Ferguson DJ, White NJ: An ultrastructural study of the brain in fatal Plasmodium falciparum malaria. Am J Trop Med Hyg 2003, 69: 345–359
10. Armah H, Dodoo AK, Wiredu EK, Stiles JK, Adjei AA, Gyasi RK, Tettey Y: High-level cerebellar expression of cytokines and adhesion molecules in fatal, paediatric, cerebral malaria. Ann Trop Med Parasitol 2005, 99:629–647
11. Ockenhouse CF, Tegoshi T, Maeno Y, Benjamin C, Ho M, Kan KE, Thway Y, Win K, Aikawa M, Lobb RR: Human vascular endothelial cell adhesion receptors for Plasmodium falciparum-infected erythrocytes: roles for endothelial leukocyte adhesion molecule 1 and vascular cell adhesion molecule 1. J Exp Med 1992, 176:1183–1189
12. Turner GDH, Morrison H, Jones M, Davis TME, Looareesuwan S, Buley ID, Gatter KC, Newbold CI, Pukritayakamee S, Nagachinta B, White NJ, Berendt AR: An immunohistochemical study of the pathology of fatal malaria: evidence for widespread endothelial activation and a potential role for intercellular adhesion molecule-1 in cerebral sequestration. Am J Pathol 1994, 145:1057–1069
13. Brown H, Hien TT, Day N, Mai NT, Chuong LV, Chau TT, Loc PP, Phu NH, Bethell D, Farrar J, Gatter K, White N, Turner G: Evidence of blood-brain barrier dysfunction in human cerebral malaria. Neuropathol Appl Neurobiol 1999, 25:331–340
14. Tripathi AK, Sullivan DJ, Stins MF: Plasmodium falciparum-infected erythrocytes increase intercellular adhesion molecule 1 expression on brain endothelium through NF-kappaB. Infect Immun 2006, 74: 3262–3270
15. Tripathi AK, Sullivan DJ, Stins MF: Plasmodium falciparum-infected erythrocytes decrease the integrity of human blood-brain barrier endothelial cell monolayers. J Infect Dis 2007, 195:942–950
16. Armah H, Wired EK, Dodoo AK, Adjei AA, Tettey Y, Gyasi R: Cytokines and adhesion molecules expression in the brain in human cerebral malaria. Int J Environ Res Public Health 2005, 2:123–131
17. Deininger MH, Kremsner PG, Meyermann R, Schluesener HJ: Differential cellular accumulation of transforming growth factor-beta1, -beta2, and -beta3 in brains of patients who died with cerebral malaria. J Infect Dis 2000, 181:2111–2115
18. Haldar K, Murphy SC, Milner DA, Taylor TE: Malaria: mechanisms of erythrocytic infection and pathological correlates of severe disease. Annu Rev Pathol 2007, 2:217–249
19. Lyke KE, Burges R, Cissoko Y, Sangare L, Dao M, Diarra I, Kone A, Harley R, Plowe CV, Doumbo OK, Sztein MB: Serum levels of the proinflammatory cytokines interleukin-1 beta (IL-1beta): IL-6, IL-8, IL-10, tumor necrosis factor alpha, and IL-12(p70) in Malian children with severe Plasmodium falciparum malaria and matched uncomplicated malaria or healthy controls. Infect Immun 2004, 72:5630–5637
20. Maneerat Y, Pongponratn E, Viriyavejakul P, Punpoowong B, Looareesuwan S, Udomsangpetch R: Cytokines associated with pathology in the brain tissue of fatal malaria. Southeast Asian J Trop Med Public Health 1999, 30:643–649
21. Ringwald P, Peyron F, Vuillez JP, Touze JE, Le Bras J, Deloron P: Levels of cytokines in plasma during Plasmodium falciparum malaria attacks. J Clin Microbiol 1991, 29:2076–2078
22. Udomsangpetch R, Chivapat S, Viriyavejakul P, Riganti M, Wilairatana P, Pongponratin E, Looareesuwan S: Involvement of cytokines in the histopathology of cerebral malaria. Am J Trop Med Hyg 1997, 57:501–506
23. Vogetseder A, Ospelt C, Reindl M, Schober M, Schmutzhard E: Time course of coagulation parameters, cytokines and adhesion molecules in Plasmodium falciparum malaria. Trop Med Int Health 2004, 9:767–773
24. Burgmann H, Hollenstein U, Wenisch C, Thalhammer F, Looareesuwan S, Graninger W: Serum concentrations of MIP-1 alpha and interleukin-8 in patients suffering from acute Plasmodium falciparum malaria. Clin Immunol Immunopathol 1995, 76:32–36
25. Ochiel DO, Awandare GA, Keller CC, Hittner JB, Kremsner PG, Weinberg JB, Perkins DJ: Differential regulation of beta-chemokines in children with Plasmodium falciparum malaria. Infect Immun 2005, 73:4190–4197
26. Taylor TE, Fu WJ, Carr RA, Whitten RO, Mueller JS, Fosiko NG, Lewallen S, Liomba NG, Molyneux ME: Differentiating the pathologies of cerebral malaria by postmortem parasite counts. Nat Med 2004, 10:143–145
27. Rosner B: Fundamentals of Biostatistics. New York, Duxbury Press, 1995
28. Tedeschi CG: Neuropathology, Methods and Diagnosis. Boston, London, Little, Brown, Churchill, 1970, pp 113–115
29. Sherriff FE, Bridges LR, Gentleman SM, Sivaloganathan S, Wilson S: Markers of axonal injury in post mortem human brain. Acta Neuropathol 1994, 88:433–439
30. Umehara F, Abe M, Koreeda Y, Izumo S, Osame M: Axonal damage revealed by accumulation of beta-amyloid precursor protein in HTLV-I-associated myelopathy. J Neurol Sci 2000, 176:95–101
31. Hortobagyi T, Wise S, Hunt N, Cary N, Djurovic V, Fegan-Earl A, Shorrock K, Rouse D, Al-Sarraj S: Traumatic axonal damage in the brain can be detected using beta-APP immunohistochemistry within 35 min after head injury to human adults. Neuropathol Appl Neurobiol 2007, 33:226–237
32. Kwon EE, Prineas JW: Blood-brain barrier abnormalities in longstanding multiple sclerosis lesions: an immunohistochemical study. J Neuropathol Exp Neurol 1994, 53:625–636
33. Newton CR, Crawley J, Sowumni A, Waruiru C, Mwangi I, English M, Murphy S, Winstanley PA, Marsh K, Kirkham FJ: Intracranial hypertension in Africans with cerebral malaria. Arch Dis Child 1997, 76: 219–226
34. Waller D, Crawley J, Nosten F, Chapman D, Krishna S, Craddock C, Brewster D, White NJ: Intracranial pressure in childhood cerebral malaria. Trans R Soc Trop Med Hyg 1991, 85:362–364
35. Walker O, Salako LA, Sowunmi A, Thomas JO, Sodeine O, Bondi FS: Prognostic risk factors and post mortem findings in cerebral malaria in children. Trans R Soc Trop Med Hyg 1992, 86:491–493
36. Newton CR, Peshu N, Kendall B, Kirkham FJ, Sowunmi A, Waruiru C, Mwangi I, Murphy SA, Marsh K: Brain swelling and ischaemia in Kenyans with cerebral malaria. Arch Dis Child 1994, 70:281–287
37. Oo MM, Aikawa M, Than T, Aye TM, Myint PT, Igarashi I, Schoene WC: Human cerebral malaria: a pathological study. J Neuropathol Exp Neurol 1987, 46:223–231
38. Craig A, Scherf A: Molecules on the surface of the Plasmodium falciparum infected erythrocyte and their role in malaria pathogenesis and immune evasion. Mol Biochem Parasitol 2001, 115:129–143
39. Tripathi AK, Sha W, Shulaev V, Stins MF, Sullivan DJ Jr: Plasmodium falciparum-infected erythrocytes induce NF-kappaB regulated inflammatory pathways in human cerebral endothelium. Blood 2009, 114:4243–4252
40. Bevilacqua MP, Pober JS, Majeau GR, Cotran RS, Gimbrone MA Jr: Interleukin 1 (IL-1) induces biosynthesis and cell surface expression of procoagulant activity in human vascular endothelial cells. J Exp Med 1984, 160:618–623
41. Nachman RL, Hajjar KA, Silverstein RL, Dinarello CA: Interleukin 1 induces endothelial cell synthesis of plasminogen activator inhibitor. J Exp Med 1986, 163:1595–1600
42. Nawroth PP, Stern DM: Modulation of endothelial cell hemostatic properties by tumor necrosis factor. J Exp Med 1986, 163:740–745
43. Schorer AE, Kaplan ME, Rao GH, Moldow CF: Interleukin 1 stimulates endothelial cell tissue factor production and expression by a prostaglandin-independent mechanism. Thromb Haemost 1986, 56:256–259
44. Pino P, Vouldoukis I, Kolb JP, Mahmoudi N, Desportes-Livage I, Bricaire F, Danis M, Dugas B, Mazier D: Plasmodium falciparum–infected erythrocyte adhesion induces caspase activation and apoptosis in human endothelial cells. J Infect Dis 2003, 187:1283–1290
45. Toure FS, Ouwe-Missi-Oukem-Boyer O, Bisvigou U, Moussa O, Rogier C, Pino P, Mazier D, Bisser S: Apoptosis: a potential triggering mechanism of neurological manifestation in Plasmodium falciparum malaria. Parasite Immunol 2008, 30:47–51

46. Wassmer SC, Combes V, Candal FJ, Juhan-Vague I, Grau GE: Platelets potentiate brain endothelial alterations induced by Plasmodium falciparum. Infect Immun 2006, 74:645–653
47. Brown H, Rogerson S, Taylor T, Tembo M, Mwenechanya J, Molyneux M, Turner G: Blood-brain barrier function in cerebral malaria in Malawian children. Am J Trop Med Hyg 2001, 64:207–213
48. Susomboon P, Maneerat Y, Dekumyoy P, Kalambaheti T, Iwagami M, Komaki-Yasuda K, Kawazu S, Tangpukdee N, Looareesuwan S, Kano S: Down-regulation of tight junction mRNAs in human endothelial cells co-cultured with Plasmodium falciparum-infected erythrocytes. Parasitol Int 2006, 55:107–112
49. Huynh HK, Dorovini-Zis K: Effects of interferon-gamma on primary cultures of human brain microvessel endothelial cells. Am J Pathol 1993, 142:1265–1278
50. Wong D, Dorovini-Zis K, Vincent SR: Cytokines, nitric oxide, and cGMP modulate the permeability of an in vitro model of the human blood-brain barrier. Exp Neurol 2004, 190:446–455
51. Hunt NH, Grau GE: Cytokines: accelerators and brakes in the pathogenesis of cerebral malaria. Trends Immunol 2003, 24:491–499
52. Malaguarnera L, Musumeci S: The immune response to Plasmodium falciparum malaria. Lancet Infect Dis 2002, 2:472–478
53. Silamut K, Phu NH, Whitty C, Turner GD, Louwrier K, Mai NT, Simpson JA, Hien TT, White NJ: A quantitative analysis of the microvascular sequestration of malaria parasites in the human brain. Am J Pathol 1999, 155:395–410
54. Floris S, Ruuls SR, Wierinckx A, van der Pol SM, Dopp E, van der Meide PH, Dijkstra CD, De Vries HE: Interferon-beta directly influences monocyte infiltration into the central nervous system. J Neuroimmunol 2002, 127:69–79
55. Lawson C, Wolf S: ICAM-1 signaling in endothelial cells. Pharmacol Rep 2009, 61:22–32
56. Schwarzer E, Skorokhod OA, Barrera V, Arese P: Hemozoin and the human monocyte: a brief review of their interactions. Parassitologia 2008, 50:143–145
57. Adamson P, Etienne S, Couraud PO, Calder V, Greenwood J: Lymphocyte migration through brain endothelial cell monolayers involves signaling through endothelial ICAM-1 via a rho-dependent pathway. J Immunol 1999, 162:2964–2973
58. Jain V, McClintock S, Nagpal AC, Dash AP, Stiles JK, Udhayakumar V, Singh N, Lucchi NW: Macrophage migration inhibitory factor is associated with mortality in cerebral malaria patients in India. BMC Res Notes 2009, 2:36
59. Shao D, Han Z, Lin Y, Zhang L, Zhong X, Feng M, Guo Y, Wang H: Detection of Plasmodium falciparum derived macrophage migration inhibitory factor homologue in the sera of malaria patients. Acta Trop 2008, 106:9–15
60. Bernhagen J, Krohn R, Lue H, Gregory JL, Zernecke A, Koenen RR, Dewor M, Georgiev I, Schober A, Leng L, Kooistra T, Fingerle-Rowson G, Ghezzi P, Kleemann R, McColl SR, Bucala R, Hickey MJ, Weber C: MIF is a noncognate ligand of CXC chemokine receptors in inflammatory and atherogenic cell recruitment. Nat Med 2007, 13:587–596